IMPACT OF PROPELLER EMERGENCE ON HULL, PROPELLER, ENGINE, AND FUEL CONSUMPTION PERFORMANCE IN REGULAR HEAD WAVES

Mohammad Hossein Ghaemi [ID]*
Gdansk University of Technology, Faculty of Mechanical Engineering and Ship Technology, Poland
Hamid Zeraatgar [ID]
Amirkabir University of Technology, Faculty of Maritime Technology, Iran
* Corresponding author: *ghaemi@pg.edu.pl (M. H. Ghaemi)*

ABSTRACT

In this study, the impact of propeller emergence on the performance of a ship (speed), propeller (thrust, torque, and RPM), a diesel engine (torque and RPM) and fuel consumption are analysed under severe sea conditions. The goal is to describe the variation in the system variables and fuel consumption rather than analysing the motion of the ship or the phenomenon of propeller ventilation in itself. A mathematical model of the hull, propeller, and engine interactions is developed in which the propeller emergence is included. The system parameters are set using model experiments, empirical formulae, and available data for the engine. The dynamic response of the system is examined in regular head waves under submerged and emerged conditions of the propeller. The pulsatility and the extent of variation of 20 selected variables for the coupled system of hull, propeller, and engine are elaborated using quantitative and qualitative terms and absolute and relative scales. The simulation begins with a ship moving on a straight path, in calm water, with a constant speed for the ship, propeller and engine under steady conditions. The ship then encounters regular head waves with a known time series of the total resistance of the ship in waves. Large motions of the ship create propeller emergence, which in turn reduces the propeller thrust and torque. This study shows that for a specific ship, the mean ship speed, shaft angular velocity, and engine power were slightly reduced in submerged conditions with respect to calm water. We compared the mean values of the variables to those in the emerged condition, and found that the shaft angular velocity was almost the same, the ship speed was considerably reduced, and the engine power significantly dropped with respect to calm water. The ratios of the amplitude of fluctuation to the mean (Amp/Mean) for the ship speed and angular velocity of the shaft under both conditions were considerable, while the Amp/Mean for the power delivered by the engine was extremely high. The outcomes of the study show the degree of influence of propeller emergence on these variables. We identify the extent of each change and categorise the variables into three main groups based on the results.

Keywords: Ship dynamics, Ship Propulsion system, Propeller ventilation, Propeller emergence, Sea waves

INTRODUCTION

A conventional ship propulsion system includes one or more propellers, a power transmission shaft, a gearbox (if any), and one or more engines, which interact with the ship's hull. The performance of the hull and that of the propulsion system are coupled, and are affected by the environmental conditions. Low and moderate sea waves generally cause moderate dynamic motion. Although propeller ventilation and the resulting load variations may happen under fully submerged conditions, propeller emergence leads to a rapid oscillation in the propeller torque demand, and consequently disturbs the engine torque supply. This may cause frequent overloading of the engine. Cyclic loading such as this can impose defects on the power transmission shaft, bearings, coupling elements, the engine and its subsystems, such as cooling or lubrication systems. Depending on the height and period of the waves, the resulting load oscillation can

increase fuel consumption and emissions [1]. An analysis of this phenomenon involves considering the overall interactions between the propeller, hull, and engine in response to external disturbances [2]. There are also other aspects that are coupled with these interactions: in case of the propeller, cavitations, [3, 4], vibrations [5], and tip vortices [6] are phenomena that affect these interactions. The interaction between the propeller and the rudder and the influence of the blade pitch on the hydrodynamic performance of propeller [7] are other aspects that should be mentioned in this regard. Last but not least, the configuration of propeller, for example with or without a Wake-Equalising Duct (WED) [8], changes the performance of the propeller and the interactions mentioned above.

Propeller emergence in severe sea waves may cause the engine subsystems, the engine itself, and the ship as a whole to fail. The goal of this study is therefore to analyse the effect of propeller emergence by combining the performance of the hull, propeller, and engine and their interactions into one overall approach. For this purpose, a suitable mathematical model is developed and the parameters are identified to reflect a real case, based on the results of experimental model tests, and a simulation is then carried out.

We present an intensive investigation of the phenomenon of propeller ventilation, its inception and mechanism, and its influence on propeller thrust and torque, depending on the operational conditions in terms of sea waves. Our results are mainly based on model experiments, CFD techniques, simulations, and analytical analyses.

Koushan [9] previously conducted an experimental study on the dynamics of the propeller blade and duct loading fluctuations and the ventilation phenomenon of thrusters in dynamic positioning (DP) mode, using dynamic model tests of a ducted pushing thruster and an open pulling thruster. He extended his research through the use of model tests of a ducted pushing thruster and an open pulling thrusters, under both constant immersion and with a forced sinusoidal heave motion under bollard conditions. Kozlowska et al. [10] analysed Koushan's [9] experiments and devised a classification for different types of propeller ventilation, with the typical thrust loss related to each of them, and presented a discussion on the ventilation inception mechanism. Koushan et al. [11] considered the influence of wave-induced propeller ventilation on the fluctuations in the propeller thrust through high-precision experimental tests with different immersion ratios and under different types of regular waves with a range of advance speeds. Califano and Steen [12] utilised RANS to carry out a numerical simulation of propeller ventilation and compared their results with those of experiments conducted by Koushan [9]. They presented a detailed description of the ventilation mechanism.

Palm et al. [13] employed model tests and CFD tools to study the ventilation characteristics of a rudder propeller in comparison to a Voith Schneider propeller. Koushan et al. [14] considered the forces and moments acting on a single propeller blade running in ventilated conditions in calm water and waves using model tests. They analysed the influence of static immersion, wave height, wave period, and propeller loading

on forces and moments. Kozlowska et al. [15] investigated the forces acting on a propeller during ventilation, and compared the blade forces and moments during the non-ventilating and ventilating phases using a model test and CFD simulation.

Paik [16] analysed the performance of a partially submerged propeller in bollard conditions, using CFD tools based on a RANS code, for different angular velocities and submerged depths of the propeller. Yvin et al. [17] conducted a full-scale CFD-based simulation of the ventilation phenomenon based on model tests of a pushing thruster. They developed a clear and exact calculation method for detecting the inception of propeller ventilation, and identified the challenges in terms of numerical evaluation of the thrust and torque losses in a partially or highly ventilated regime. Kozłowska [18] conducted model tests and numerical simulations of propeller ventilation in waves and partially submerged conditions. She analysed the mean thrust, torque, and thrust loss as a function of the blade position, and explored the influence of time on the inception of ventilation. She also suggested a calculation model for propeller thrust and torque diminution factor. Kozlowska et al. [19] studied the dynamic effects on propeller loading during ventilation. They investigated the propeller forces under varying operational conditions for both steady and unsteady states. The performance of the propeller, hull, and engine in sea waves is another area of research in which many studies have previously been conducted. Lanchukovsky [20] investigated the effects of moderate and severe wave on the performance of the propeller and engine, and demonstrated that in rough seas, propeller emergence due to large ship motions causes a loss of propeller torque. Szelangiewicz and Żelazny [21] put forward a method for predicting the influence of propeller emergence and the thrust reduction during navigation of a ship in waves. Szelangiewicz and Żelazny [22] also presented an algorithm for calculating the drop in propeller torque during ship motion in irregular waves under propeller emergence conditions. Theotokatos and Tzelepis [23] simulated the interactions between the hull, propeller and engine, and applied a simulation method to explore the engine performance and emissions. They analysed the behaviour of the propulsion system for a given range of sea waves and a particular route. Taskar [24] proposed a coupled model consisting of an engine, hull and propeller for wake estimation in waves. They compared the propulsion performance of a ship under steady and unsteady conditions and showed that these may be significantly different. The most important outcome of this study was the conclusion that the response of the system, including the engine power, propeller rotation speed and torque, can be determined only through the use of a coupled simulation model when realistic engine and propeller models are employed. Following this, Tokgoz et al. [25] carried out experimental and numerical analyses of twin propellers operating behind a hull in regular head wave conditions. They concluded that in regular waves, and at an encounter frequency close to its mean value in calm water, the propeller thrust undergoes harmonic oscillation, with a relatively small amplitude; however, when the propeller blade approaches the water surface and ventilation occurs, the

propeller thrust radically changes and decreases. Kitagawa et al. [26] considered the influence of wave orbital motion on the propeller inflow velocity and engine load fluctuations in waves. Free-running model tests in head waves driven by a servo-motor were employed to provide data for analysis.

Under rough sea conditions, the propeller may undergo large vertical motions, and the propeller disc is sometimes exposed above the surface of the water. An abrupt drop in torque can be found, which is proportional to the loss of the effective propeller disc area due to exposure above the free surface. These effects have been carefully analysed and discussed by Naito [27], Minsaas et al. [28], Minsaas et al. [29], Koushan [30], Smogeli [31], and Oleksiy and Masashi [32]. A detailed investigation of the propeller and propulsion performance, as well as the propulsive coefficients in waves, has recently been carried out by Saettone [33].

In [34], a mathematical model of the interactions between the hull, propeller, and engine was developed. In [35], the authors investigated the dynamics of a ship propulsion system in sea waves, including the interactions between the hull, propeller, and engine in low and moderate sea waves. Propeller ventilation was not the topic of this study.

The present work is in line with these previous studies, and represents a step forward in dealing with conditions where propeller ventilation occurs. The main goal of the study is to analyse the impacts of propeller ventilation on the ship and propeller speed and the performance of the main engine. The sub-systems of the main engine are also monitored during ventilation, and the ventilation characteristics are determined through the use of existing regression formulae. Our approach takes into consideration the internal engine variables through the use of an instantaneous value zero-dimensional mathematical model for the diesel engine. The influence of the wave orbital velocity on the propeller inflow velocity is also included. The simulation represents a specific ship, and the parameters are identified based on the results of model tests of the propeller and ship. The output includes the dynamic behaviour of the ship and time traces for the engine and its variables during propeller ventilation.

The results of this study provide a general overview of the impact of propeller ventilation on the general performance of the whole propulsion system. The results are quantitatively and qualitatively analysed to determine the extent of the variation in each variable. This study is the first attempt to investigate the effect of propeller emergence on the elements of a propulsion system while taking their interactions into consideration. It should be noted that the main goal here is not to study the phenomenon of propeller ventilation itself but to focus on its impact on the ship propulsion system.

MATHEMATICAL MODEL

COUPLED EQUATIONS FOR A FULLY SUBMERGED PROPELLER IN REGULAR WAVES

A review of the model used to represent the interactions between the hull, propeller, and engine is presented in this section, and further details are available in [35]. The dynamics of the hull, propeller and diesel engine are interrelated, particularly during operation in sea waves. The following two coupled equations govern the relationships between them:

$$\begin{cases} -R_T(u(t)) - R_a(t) + T_n(t) = (\Delta + x_{\dot{u}})\,\dot{u}(t) \\ Q_E(t) - Q_P(t) = (I_P + I_{Pa} + I_E + I_S)\,\dot{\omega}(t) \end{cases} \quad \text{(1)}$$

where $T_n(t)$ is the net thrust generated by the propeller as a function of time, $R_T(u(t))$ is the ship resistance as a function of surge speed, $R_a(t)$ is the total wave force in the x-direction, a mean value is used as the added resistance, Δ is the overall ship mass, $x_{\dot{u}}$ is the surge added mass, and u and $\dot{u}$ are surge velocity and acceleration, respectively. $Q_E(t)$ is the torque delivered by the engine, $Q_P(t)$ is the propeller torque demand, $\dot{\omega}(t)$ is the angular acceleration of the propeller, and I_P, I_{Pa}, I_E, and I_S are the moment of inertia and added moment of inertia of the propeller, the moment of inertia of the engine, and the moment of inertia of the shaft, respectively.

Ship resistance
The ship resistance can be calculated by empirical methods, numerical methods, or based on a model test, and can be expressed as follows:

$$R_T(u(t)) = \frac{1}{2}C_T\rho\,u^2(t)A_s \quad \text{(2)}$$

where C_T is the total resistance coefficient, ρ is the water density, and A_s is the wetted surface area.

Surge added mass
The surge added mass $x_{\dot{u}}$ is typically as assumed to be between 5% and 10% of a ship's mass [36, 37]. In this study, we assume a value of 10%.

Wave force
The mean value of the wave force in the x-direction as the added resistance and its time history can be approximated by numerical methods or by using a model test. For the latter, the total resistance of the model in a given regular wave is recorded as a function of time, as $R_{tm}(t)$. From the total resistance of the model in calm water at a given speed u, $R_{Tm}(u(t))$, the time history of the wave force of the model, $R_{am}(t)$, can be calculated as follows:

$$R_{am}(t) = R_{tm}(t) - R_{Tm}(u(t)) \qquad (3)$$

where the subscripts *m, T,* and *t* refer to the model, total value, and time, respectively.

The time history of the wave force on the ship, $R_a(t)$, can be calculated as follows:

$$R_a(t) = \lambda^3 \cdot R_{am}(t) \qquad (4)$$

where λ is the model scale.

Propeller torque and thrust

A screw propeller with an instantaneous rotational speed of $n(t)$ and advance speed $u_A(t)$ generates a thrust of $T(t)$, and demands torque $Q_P(t)$. Although the propeller is in the acceleration mode, the thrust and torque are approximately determined by using the open water performance of the propeller in the steady condition, for the sake of simplicity, as follows:

$$J_A(t) = \frac{u_A(t)}{D_p |n_P(t)|} \qquad (5)$$

$$T(t) = K_T(J_A(t)) \rho n_P(t) |n_P(t)| D_P^4 \qquad (6)$$

$$Q_P(t) = K_Q(J_A(t)) \rho n_P(t) |n_P(t)| D_P^5 \qquad (7)$$

where $K_T(t)$ and $K_Q(t)$ are the propeller thrust and torque coefficients, respectively, n_P is the rotational speed of the propeller expressed in rps, and D_P is the diameter of the propeller.

The net thrust, $T_n(t)$, depends on the thrust deduction factor, $t_T(t)$:

$$T_n(t) = T(t)(1 - t_T(t)) \qquad (8)$$

The wake fraction coefficient and thrust deduction factor are functions of time when the ship is sailing in sea waves. For the sake of simplicity, they can be approximated to the same values as in the steady state, determined based on empirical formulae. Examples are given below:

$$w = 0.45 C_p - 0.05 \quad \text{(Robertson)} \qquad (9)$$

$$t_T = 0.5 C_p - 0.12 \quad \text{(Hecker)} \qquad (10)$$

where C_p is the hull prismatic coefficient ([35], Table 2).

The surge and wave orbital inflow velocities are also included in the model, and these are presented in Appendix A.

DIESEL ENGINE

Under high wave conditions, the propeller may experience a diminution of thrust and torque due to exposure of the propeller disc above the free surface [28]. This large and abrupt drop in torque may lead to engine over-speed, which is known as propeller racing [25]. The resulting change in the propeller torque is proportional to the loss of the effective disc area of the propeller. From [28], if K_{T0} and K_{Q0} are the thrust and torque coefficients for a fully-submerged propeller, then for limited immersion at the same advance number (J_0), these become:

$$K_T = \beta \cdot K_{T0} \qquad (11)$$

$$K_Q = \beta^m \cdot K_{Q0} \qquad (12)$$

where m is assumed to be a constant between 0.80 and 0.85 [20]. Another related study suggests a value of one for m [30]. It should be noted that the emerged portion of the propeller is only responsible for part of the losses. For a high advance number, neglecting other effects is reasonable, otherwise the effect of ventilation can be much more severe than the emerged portion of the propeller. This is examined and discussed in [14] and [19]. Since the advance number is relatively high in this study, only the emerged portion of the propeller is included in our analysis.

The thrust diminution factor, β, depends on the advance number, which can be calculated based on the geometrical relationships (see Fig. 1) as a fraction of the emerged area of the propeller disk (S) over its overall area (S_0):

$$\beta = \frac{S}{S_0} \qquad (13)$$

or:

$$\beta = real\left(1 - \frac{acos\, \varepsilon}{\pi} + \frac{\varepsilon}{\pi}\sqrt{1 - \varepsilon^2}\right) \qquad (14)$$

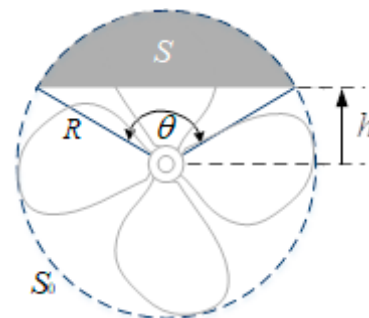where $\varepsilon = \frac{h}{R}$, h is the propeller immersion, and R is the propeller radius.

Fig. 1. Definition of parameters for a partially immersed propeller

There are three other methods of approximating the thrust diminution factor, as presented in [23], [32] and [18], and these are described in Appendix C.

For unsteady state conditions, ε should be expressed as a function of time. This requires calculating h depending on six variables, three of which are related to the motion of the ship (heave, roll, and pitch) and three to the sea condition (wave amplitude, frequency, and heading angle). It can be formulated as shown in the following equation, based on the dynamics of the ship's hull as a rigid body:

$$h(x, y, \mu, t) = \eta_3(t) + y \cdot \eta_4(t) - x \cdot \eta_5(t) - \zeta(x, y, \mu, t) \quad (15)$$

where η_3, η_4 and η_5 are the heave, roll, and pitch, respectively, and the related phases are φ_3, φ_4 and φ_5 (see Fig. 2):

$$\eta_3(t) = \bar{\eta}_3 \cos(\omega_e t + \varphi_3) \quad (16)$$

$$\eta_4(t) = \bar{\eta}_4 \cos(\omega_e t + \varphi_4) \quad (17)$$

$$\eta_5(t) = \bar{\eta}_5 \cos(\omega_e t + \varphi_5) \quad (18)$$

and ζ represents the wave profile, as follows:

$$\zeta(x, y, \mu, t) = \bar{\zeta} \cos(kx \cos\mu + ky \sin\mu - \omega_e t) \quad (19)$$

Here, k is the wavenumber, μ is the heading angle and ω_e is the encounter frequency, which is defined as follows:

$$\omega_e(t) = \omega(t) - ku(t) \cos\mu \quad (20)$$
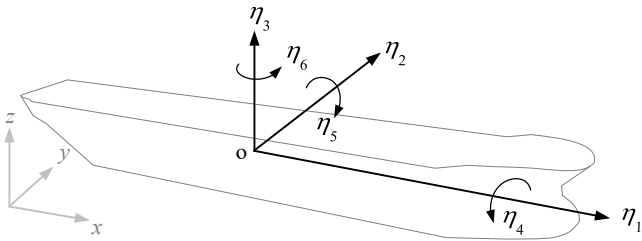
Under head sea conditions, $\mu = \pi$ and $y = 0$.

Fig. 2. Motion of the ship in the hydrodynamic coordinate system: η_1: surge, η_2: sway, η_3: heave, η_4: roll, η_5: pitch, η_6: yaw

To include the propeller ventilation and wave orbital velocity in the mathematical model, we recall the system of coupled equations in Eq. (1). The terms $T_n(t)$ and $Q_P(t)$ are evaluated taking into consideration the propeller emergence, as formulated above, and the wave orbital velocity, which is given in Appendix A.

CASE STUDY AND SIMULATION

CASE STUDY

We consider a case based on the same container vessel as used in previous studies [34, 35]. This allows us to compare the performance of a fully submerged propeller with a ventilated propeller when the wave conditions are similar in both simulations.

Specifications of the ship and propeller

The parameters for the ship and the propeller are given in Table 1 and Table 2, respectively. The arrangement of the propeller behind the hull is illustrated in Fig. 3.

Tab. 1. Ship specifications [34]

No.	Parameter	Symbol	Value
1	Displacement	Δ	26980.220 [ton]
2	Wet length Length BP	L_{WL} L_{BP}	186.260 [m] 182.880 [m]
3	Beam	B	24.414 [m]
4	Draught	T	9.782 [m]
5	Ship speed	u	23.82 [Kn]
6	Block coefficient	C_B	0.600 [-]
7	Prismatic coefficient	C_P	0.615 [-]
8	Wetted surface	A	5762.200 [m²]

Tab. 2. Propeller specifications [34]

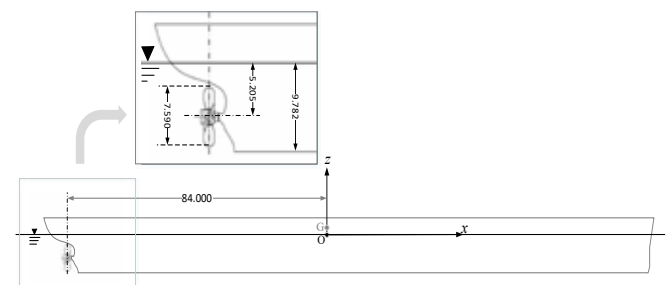| Type	B-Wageningen fixed pitch propeller
Diameter	7.590 [m]
Number of blades	5
Area ratio	0.5808
Pitch ratio	1.00 (at full pitch)

Fig. 3. Propeller immersion height and x-coordinate in calm water conditions

Wave specifications, ship motion, and added resistance

The model of the ship was previously tested in regular waves, as shown in Table 3, at a speed equivalent to the scaled ship speed. The heave and pitch motion and the total resistance were recorded. Table 4 gives the data used for the model and the ship, and Fig. 4 shows the total resistance versus the selected period in regular waves, which were 326 cm in height and 162.84 m in length. More details on the ship and propeller model tests are given in [34] and [35].

Tab. 3 . Specifications of the regular waves, L_m=4.58 m and λ=40.71 m

Case	Wave height, H [cm]	Wave period, T [s]	Wave length [m]	T_e [s]	ω_e [rad/s]
Model	8	1.60	4.00	1.005	6.25
Ship	326	10.21	162.84	6.42	0.978

Tab 4 . Heave and pitch motion displacements for the model and ship, and phase lags

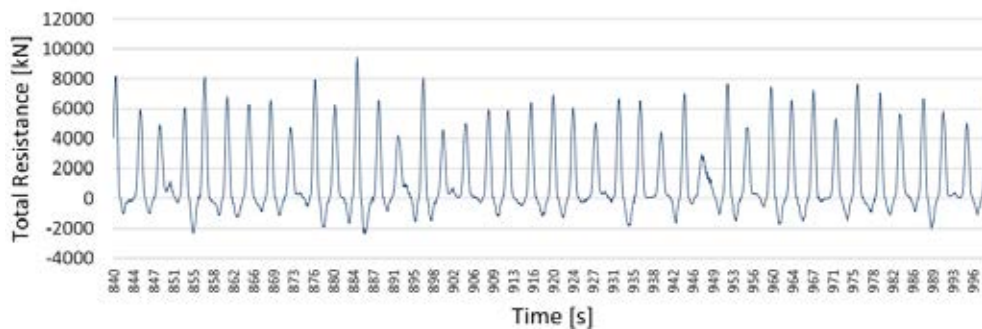| Case	Heave ampl. [cm]	Pitch ampl. [deg.]	Heave phase angle [deg.]	Pitch phase angle [s]
Model	3.6	2.4	−35	−50
Ship	156.6	2.4	−35	−50

Fig. 4. Total resistance versus time in regular waves, height 326 cm, length 162.84 m [35]

SIMULATIONS

A computer code was developed in MATLAB based on the problem formulation. The simulation was carried out based on the recorded waves and the resulting total resistance as input. The outputs were the variables for the ship, propeller, and engine, which consisted of the ship speed, shaft angular velocity, fuel consumption, fuel rate, propeller thrust and torque, engine torque and power, propeller thrust and torque diminution factor, β, as well as a set of selected flow and thermodynamic engine variables. A comparison between the time histories for a fully submerged propeller and a ventilated propeller can illustrate the significance of the impact of propeller emergence on the overall performance of the system. The simulation was initially carried out for calm water conditions for a period of 500 s, to establish the steady-state behaviour of the system. For the following (approximately) 800 s, the simulation was continued with regular waves, in which the propeller was in a ventilated condition. Finally, calm sea conditions were applied again, and all dynamic systems gradually tended towards a steady condition. The total simulation time was 1500 s.

The results for the ship and propeller variables are presented in Fig. 5 and Fig. 6, starting at *t* = 400 s for both the submerged and ventilated propeller conditions. In Fig. 5, the total resistance (which formed the main input) is plotted against the ship's speed, shaft angular velocity, net propeller thrust, propeller torque, engine torque, propeller demand power, and engine delivered power, for simulation time intervals of 400 to 1500 s.

Fig. 6 shows the results for a time frame of 50 s is which the dynamic variables regularly fluctuated. A plot of the propeller thrust and torque diminution factor, β, versus time, under sea wave conditions, is shown in Fig. 7, and the time history for some flow and thermodynamic internal variables of the engine is illustrated in Fig. 8. These include the mass and temperature of the air in the inlet air manifold (receiver), the mass and temperature of the exhaust gases in the exhaust gas receiver, and the flow rate and temperature of the exhaust gases after the turbocharger. To check the internal parameters of the engine, and particularly the combustion process, which has a strong influence on the emissions, the time variation in the average temperature of the gases during the combustion process and the temperature of the outflow gases from the engine cylinders are shown in

Fig. 9. Finally, the fuel rate and the fuel consumption for both conditions (submerged and ventilated propeller) are compared in Fig. 10.
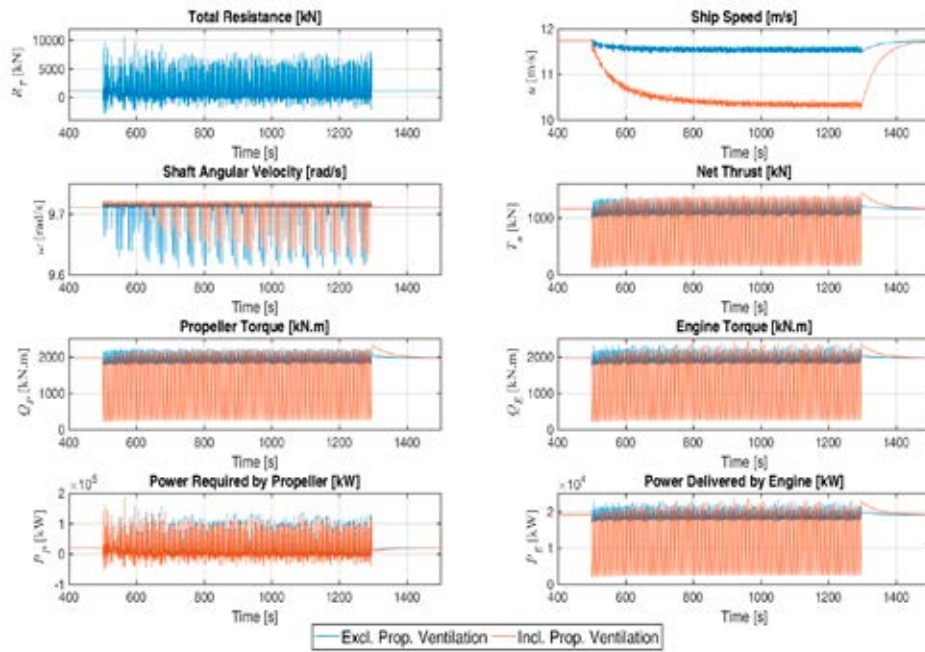
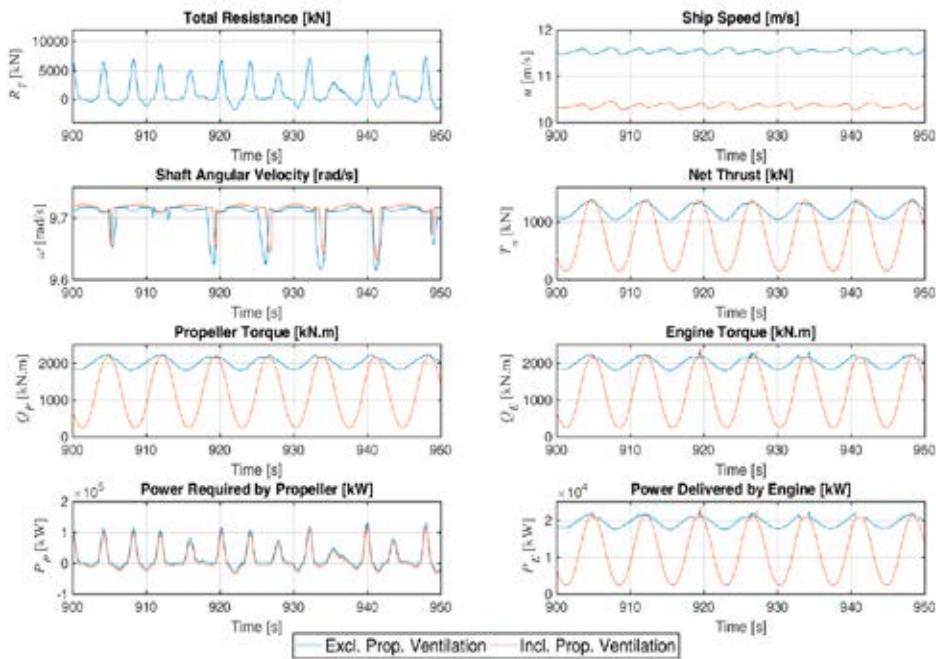*Fig. 5. Overall time history of the input total resistance and selected system variables*

Fig. 6. Time history (50 s) showing the input total resistance and selected system variables under fully submerged and ventilated conditions
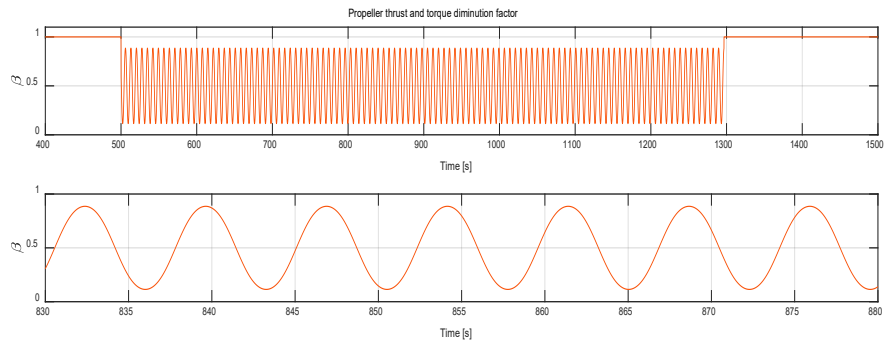
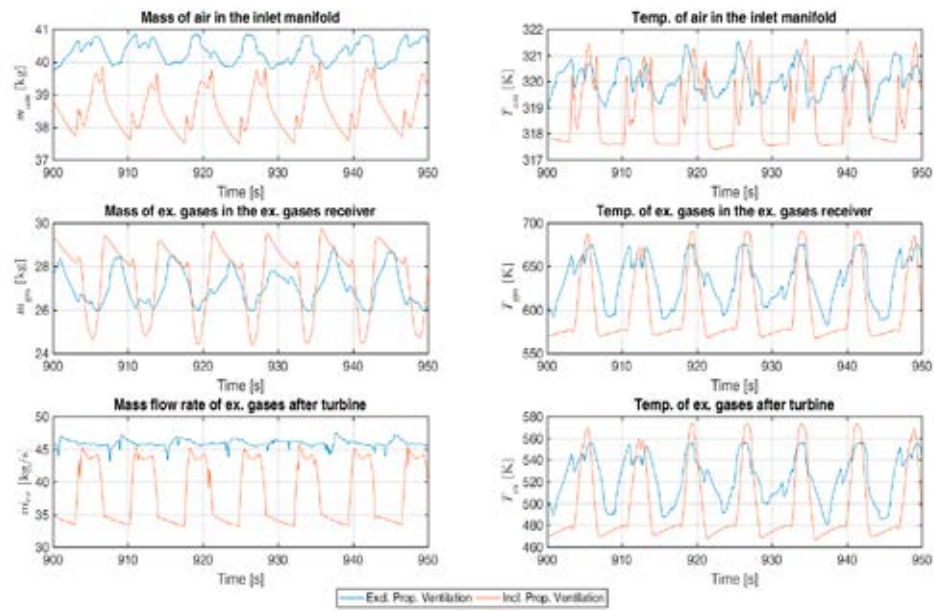*Fig. 7. Propeller thrust and torque diminution factor, β, versus time*

Fig. 8. Comparison of the behaviour of the engine variables under submerged and ventilated propeller conditions
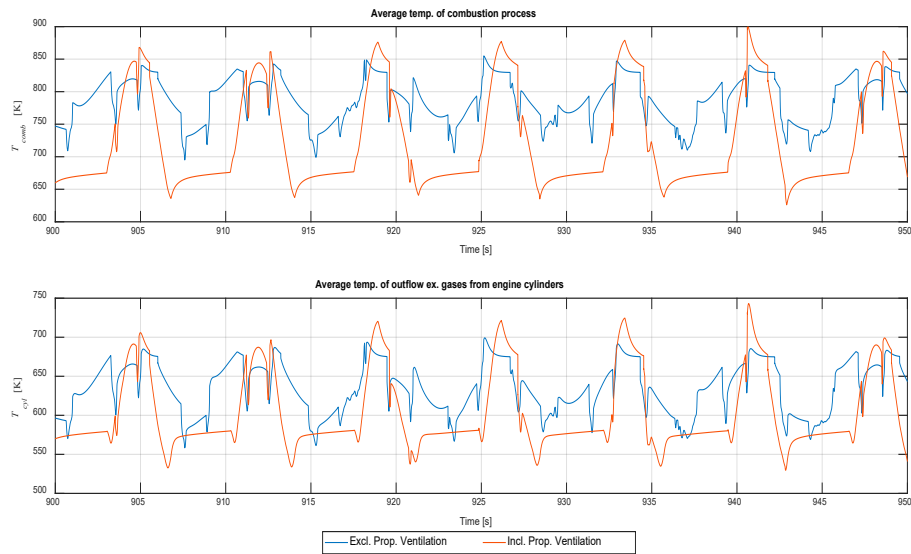

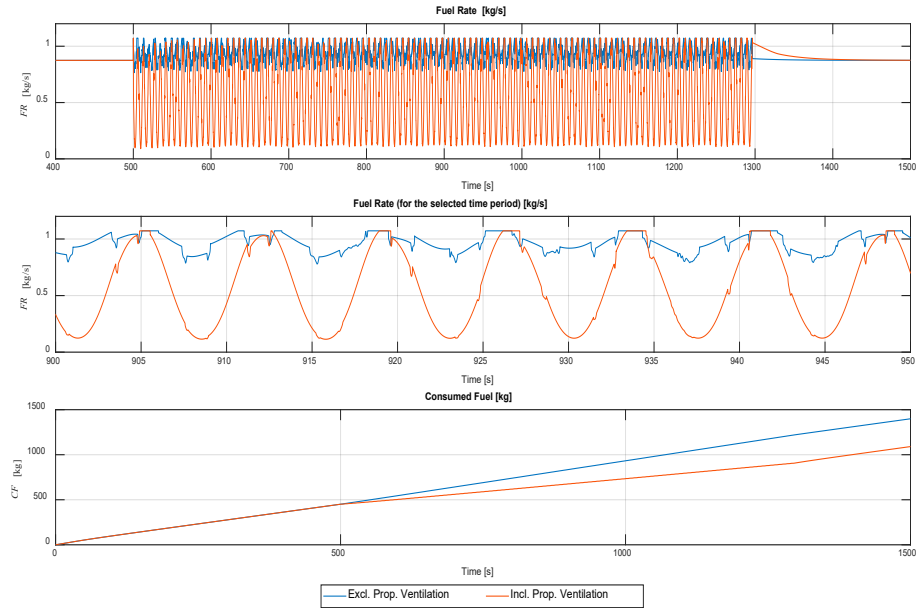*Fig. 9. Influence of propeller ventilation on the combustion process*

Fig. 10. Comparison of the variation in the fuel rate and total fuel consumed under submerged and ventilated conditions

DISCUSSION

The statistical parameters of the hull, propeller and engine were calculated and compared for both submerged and ventilated propeller conditions. For this purpose, a time frame of between 900 and 1200 s was selected during which the fluctuations of the variables were in almost a steady state.

These statistical parameters, including the maximum, minimum, amplitude, mean, and root mean square (RMS) values, and the variance for submerged and ventilated propeller conditions, are summarised in Table 5. The values are labelled as 'Ex' when the propeller ventilation is excluded from the simulations, and 'In' when it is included.

The terms 'Max' and 'Min' are defined as the maximum positive peak and minimum negative peak of a function, respectively. It should be noted that the amplitude is defined as the half of the absolute difference between the maximum and minimum values, averaged over the length of the selected time frame:

$$Amp = \frac{Max - Min}{2} \qquad (21)$$

'Mean', μ, is the average of a function integrated over time, and is defined as follows:

$$\mu = E[f(t)] = \frac{1}{T_2 - T_1} \int_{T_1}^{T_2} f(t)dt \qquad (22)$$

where [ ] is defined as an operator for the calculation of the mean value. The variance is calculated as the mean square of a function minus its mean:

$$Var(x) = E\big[(f(t) - \mu)^2\big] \qquad (23)$$

$$Var(f(t)) = \frac{1}{T_2 - T_1} \int_{T_1}^{T_2} (f(t) - \mu)^2 \, dt \qquad (24)$$

Since the variables are continuous functions in time, the RMS will be as follows:

$$RMS = \sqrt{\frac{1}{T_2 - T_1} \int_{T_1}^{T_2} (f(t))^2 \, dt} \qquad (25)$$

The term 'Amp/Mean' represents the maximum fluctuation of a function in nondimensional terms, and reflects the pulsatility of the variable. The ratio '$\sqrt{Var/Mean}$' also represents the fluctuation of a function with respect to its mean value in nondimensional terms, except that it takes into consideration an average fluctuation amplitude. This ratio is called the *coefficient of variations*; it is generally defined as the standard deviation divided by the mean value, and indicates the extent of variability.

Tab. 5. Heave and pitch motion displacements and phase lags for the model and ship

No.	Variable	Cond.	Max	Min	Amplitude	Mean	RMS	Amp/Mean	Variance	$\sqrt{Var}/Mean$
1	Total resistance [kN]	Ex	10557.584	-3011.119	6784.351	963.868	2456.305	7.039	506182	0.738
		In	10557.584	-3011.119	6784.351	963.868	2456.305	7.039	506182	0.738
2	Ship's speed [m/s]	Ex	11.791	8.996	1.398	11.540	11.540	0.121	0.002	0.004
		In	11.767	8.996	1.385	10.343	10.343	0.134	0.002	0.004
3	Shaft angular velocity [rad/s]	Ex	9.717	6.805	1.456	9.705	9.705	0.150	0.001	0.003
		In	9.721	6.805	1.458	9.713	9.713	0.150	0.000	0.000
4	Advance number [-]	Ex	0.8317	0.6009	0.1154	0.7484	0.7492	0.154	0.0012	0.046
		In	0.8317	0.6009	0.1154	0.6702	0.6711	0.172	0.0012	0.052
5	Propeller thrust and torque diminution factor [-]	Ex	1.000	1.000	0.000	1.000	547.723	0.000	1.000	1.000
		In	0.886	0.114	0.386	0.497	312.418	0.716	0.078	0.562
6	Net thrust [kN]	Ex	1541.464	455.526	542.969	1191.669	1196.225	0.456	10875	0.088
		In	1541.464	118.981	711.241	736.086	860.283	0.966	198261	0.605
7	Propeller torque [kNm]	Ex	2413.891	814.590	799.650	2002.426	2006.859	0.399	17757	0.067
		In	2413.891	206.744	1103.574	1176.865	1369.209	0.938	489716	0.595
8	Engine torque [kNm]	Ex	3330.577	1745.695	792.441	2002.428	2006.880	0.396	17837	0.067
		In	3330.577	206.323	1562.127	1176.864	1369.192	1.327	489671	0.595
9	Required brake power [kW]	Ex	185980.06	-51796.684	118888.373	19787.918	42389.041	6.008	1405267820	1.894
		In	177353.84	-52768.920	115061.384	11846.879	37970.686	9.712	1301423957	3.045
10	Delivered brake power [kW]	Ex	23299.547	16962.731	3168.408	194 31.525	19473.498	0.163	1631686	0.066
		In	23548.700	2005.711	10771.494	11424.807	13287.092	0.943	46020142	0.594
11	Mass of air in the air manifold [kg]	Ex	40.870	39.771	0.550	40.278	3460.029	0.014	0.103	0.008
		In	40.351	37.408	1.472	38.789	2628.091	0.038	0.492	0.018
12	Temp. of air in the air manifold [K]	Ex	321.6	318.4	1.6	320.0	27487.5	0.005	0.345	0.002
		In	321.6	317.3	2.2	319.5	21641.2	0.007	1.637	0.004
13	Mass of ex. gases in the ex. gases receiver [kg]	Ex	28.941	25.912	1.515	27.020	2321.937	0.056	0.565	0.028
		In	29.828	24.358	2.735	27.037	1835.028	0.101	2.806	0.062
14	Temp. of ex. gases in the ex. gases receiver [K]	Ex	674.9	582.7	46.1	633.6	54475.0	0.073	679.7	0.041
		In	690.6	566.6	62.0	614.4	41723.9	0.101	1896.2	0.071
15	Mass flow rate of ex. gases after turbine [kg/s]	Ex	47.450	43.000	2.225	45.811	3935.501	0.049	0.343	0.013
		In	45.769	33.084	6.342	40.353	2748.632	0.157	17.97	0.105
16	Temp. of ex. gases after turbine [K]	Ex	555.8	480.5	37.7	523.3	44983.7	0.072	429.7	0.040
		In	573.9	466.0	53.9	509.7	34621.5	0.106	1371.7	0.073
17	Average temp. of combustion process [K]	Ex	700.7	558.3	71.2	631.2	54294.9	0.113	1113	0.053
		In	744.9	523.4	110.7	611.0	41556.2	0.181	3007	0.090
18	Average temp. of outflow gases from engine cylinders [K]	Ex	857.0	695.0	81.0	783.1	67344.8	0.103	1303	0.046
		In	899.7	626.0	136.9	744.6	50710.4	0.184	5968	0.104
19	Fuel rate [kg/s]	Ex	1.072	0.775	0.149	0.969	532.516	0.154	0.006	0.080
		In	1.072	0.107	0.482	0.579	369.379	0.832	0.119	0.596

A comparison of the mean values in the ventilated condition with those in the submerged condition shows a 10% decrease in the ship speed, no significant change in the shaft speed, and reductions of 10% in the propeller advance number, 38% in the propeller net thrust, and 41% in the engine torque and power.

Fig. 11 shows the Amp/Mean ratio as a nondimensional measure of merit for the analysis. In general, for all of the variables considered here, larger fluctuations are observed when the propeller is in the ventilated condition in waves than in the submerged condition. In particular, the engine torque, net thrust, required and delivered brake power, fuel rate, propeller thrust and torque diminution factor differ significantly. Since the extreme fluctuation in the variables is represented by the Amp/Mean ratio, it should be noted that a very high value of this ratio, even for a very short time, may cause failure of the system. The Amp/Mean ratio of the ship speed under submerged conditions is 0.121, which changes to 0.134 in the ventilated condition, i.e. an increase of 10%. The shaft speed has an Amp/Mean ratio of 0.15 under both conditions. The changes in the ship and shaft speed in waves are moderate. The propeller advance number has an Amp/Mean of 0.154 under submerged conditions, which

changes to 0.172 in ventilated conditions, representing an increase of 12%. The Amp/Mean ratio for the propeller generated net thrust changes from 0.456 to 0.966 when the conditions change from submerged to ventilated, and this can be regarded as a high fluctuation. The same effect is seen for the propeller torque demand; the engine-generated torque has an Amp/Mean of 0.396 in submerged conditions, which changes to 1.327 in ventilated conditions, giving a large increase. It is worth mentioning that the mean value of the engine torque drops significantly under ventilated conditions, which in turn results in no exceedance of a certain limit. The same effect is seen for the engine power.

The coefficient of variation is shown in Fig. 12. It can be seen from the figure that the internal variables of the engine are less affected by propeller ventilation than the other variables. The variable that is most affected by the propeller ventilation is the required brake power, followed by the net thrust, propeller torque, engine torque, and fuel rate. It is interesting to note that the coefficients of variation for the the ship's speed and shaft angular velocity under propeller ventilation conditions have negligible values in comparison to the other variables.
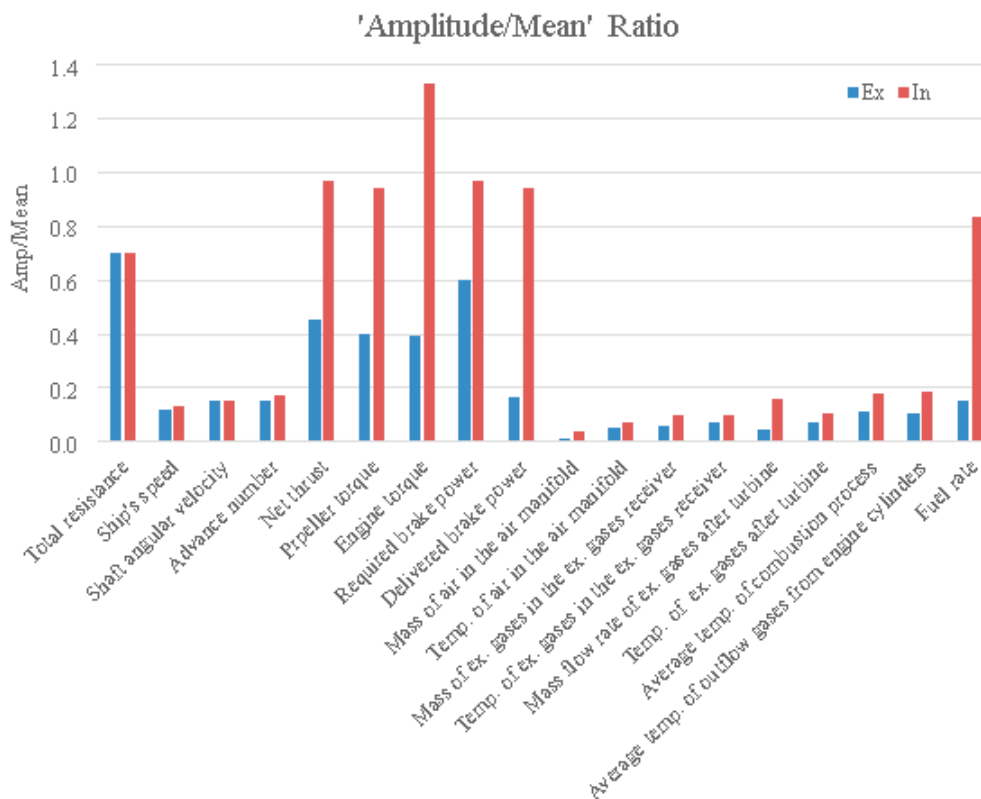

Fig. 11. Amp/Mean ratios for the system variables under submerged and ventilated conditions
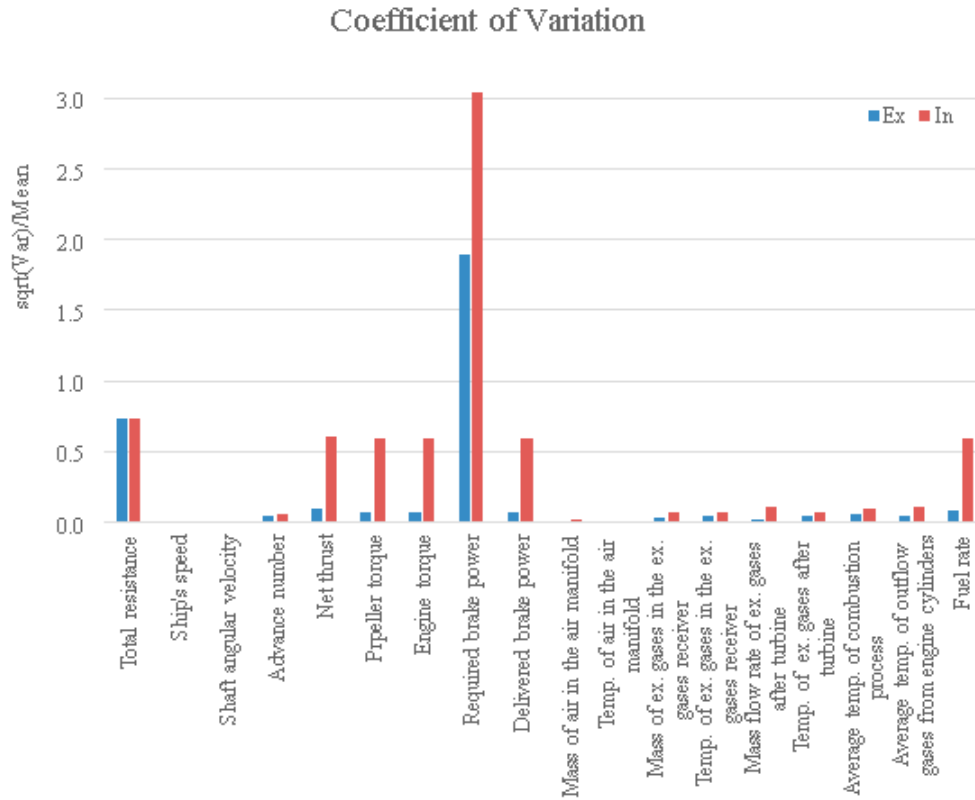
Fig. 12. Coefficients of variation for the system variables under both submerged and ventilated conditions

To allow us to analyse the results on a relative scale, the relative change ($\delta\%$) is determined as follows:

$$\delta\% = \frac{p_{In} - p_{Ex}}{p_{In}} \cdot 100 \qquad (26)$$

where p represents the statistical parameter considered (amplitude, mean, RMS, or variance), and the subscripts In and Ex refer to emergence and submergence propeller conditions. The relative changes are illustrated in Fig. 13, and it can be seen that there is a lower relative change in the mean for the variables with a higher coefficient of variation. However, for the other variables, this is RMS that has changed less, relatively. This indicates that the power of those signals that represent the internal variables of the engine remains at a lower level in comparison to the hull and propeller variables. In parallel, the relative change in the variance of the internal engine variables is higher. The shaft angular velocity shows the lowest relative change in variance, and this seems to be the result of the quick reaction of the governor, which was set for a constant angular velocity.

Fig. 13. Relative changes in the statistical parameters of the system variables (in percentages) under propeller ventilation

To carry out a qualitative comparative analysis, the relative extent of the variation in the system variables can be considered. However, the variance of the relative change for some variables is negative, and the use of the coefficient of variation is only possible when the data are positive and scaled against global axes. It is therefore necessary to add the absolute value of the highest negative value to the other values for a given statistical parameter [38]. Moreover, since the RMS is the square root of the power of a signal, it can be used as a weighting factor for this qualitative analysis. Hence,

the Qualitative Weighted Extent Variation Index, $QWEVI$, is defined and evaluated for all variables as follows:

$$QWEVI_i = CV_i \cdot \bar{\delta}_{RMS}\% \qquad (27)$$

where

$$CV_i = \frac{\sqrt{\delta_{variance}\%}}{\bar{\delta}_{mean}\%} \qquad (28)$$

$$\bar{\delta}_p = \delta_p\% + abs(min(\delta_p\%)) \qquad (29)$$

and i and p indicate the ith variable and p^{th} statistical parameter. The higher the value of $QWEVI$, the greater the extent of the variation in the variable under propeller emergence conditions. The results are illustrated in Fig. 14.

Fig. 14. Values of the qualitative weighted extent variation index (QWEVI) for selected system variables

The required brake power is demanded due to the presence of sea waves, and its $QWEVI$ is therefore expected to be among the highest. When the required brake power is excluded, there are three main groups of variables in Fig. 14. The first group with the highest $QWEVI$ values (between 32 and 33) includes the propeller torque, engine torque, delivered brake power. net thrust, and fuel rate. The second group, with moderate $QWEVI$ values of around 24, consists of the ship speed, advance number, and shaft angular velocity. The third group includes the engine flow and thermodynamic variables, for which the value of $QWEVI$ ranges between 13.1 and 17.1. WE can see that the values of $QWEVI$ for internal variables of the engine are approximately half of those for the ship and propeller variables. This does not mean that the sensitivity of the engine internal variables to the propeller ventilation is low or negligible, but indicates that the extent of the changes

concerning the other variables is important. The fuel rate is also an engine variable with a moderate value of $QWEVI$, although this is higher than the others. However, as it is an input signal for the dynamic behaviour of the engine, it should not be categorised as an internal flow variable of the engine. Since the propeller is operating in ventilation conditions, the fuel rate changes over a wide range (see Fig. 10), and the engine therefore works under a partial load for a relatively long period, giving emissions that are higher than expected for a partial load.

Table 6 shows the relative fuel consumption with respect to calm water conditions, and it can be seen that there is a 10.8% increase and 33.8% decrease in submergence and emergence conditions, respectively. However, the distance travelled and, more importantly, the mean ship speed in emergence conditions are lower than in submergence conditions. Simultaneously, the above variables in the emergence condition are lower than in the calm water condition. The required brake power is also reduced and fluctuates significantly under emergence conditions (see Fig. 10).

The mean fuel rates for both conditions (532.5 kg/s for submergence and 369.4 kg/s for emergence) given in Table 5 also confirm the above result. The Amp/Mean for the fuel rate is 0.154 and 0.832 in submergence and emergence conditions, respectively, which highlights the significance of this variation. It should be noted that in the time interval between 500 and 1200 s, when the ship is in the waves, the overall distances travelled are 8089 m and 7350 m in the submergence and emergence conditions, respectively.

Tab. 6. Comparison of the consumed fuel for two conditions

Time interval [s]	Condition	Fuel consumed (CF) [kg]	Distance travelled [m]	Ship mean speed [m/s]	Relative change in CF [%] $CF\% = \frac{CF_{EX(In)} - CF_{Calm}}{CF_{Calm}} \cdot 100$
200-500	Calm	262.49	3519	11.73	–
900-1200	Ex	290.79	3462	11.54	+10.8%
	In	173.73	3103	10.34	−33.8%

From the statistical analysis results presented in this section, it can be observed that when propeller emergence takes place, the fluctuations in the ship's speed and the engine power are significant in comparison to the other variables, and the latter also has a high pulsatility. There is also fluctuation in the propeller and engine torques, and the propeller thrust is high. The fluctuations in the ship's speed, advance number, and shaft angular velocity are at a moderate level, and the fluctuations in the internal variables of the engine, including mass, temperature, and the pressure of the air or exhaust gases in different elements of the engine and turbocharger, are relatively low.

In comparison to calm water conditions, although less fuel is consumed in the emergence condition due to a reduction in the ship speed, we observe a relatively large increase in the value of the fuel consumed per meter, from 0.074 kg/m to 0.084 kg/m (i.e. +12%). This result calls into question the control strategy of keeping the shaft angular velocity at a constant value, which is currently common practice. This strategy leads to high fluctuations in the fuel rack (fuel rate), and consequently increases the fuel consumption. The results in Table 6 highlight the importance of including the phenomenon of propeller ventilation in any analysis of the performance of a ship's propulsion system, and particularly in regard to fuel consumption.

CONCLUSIONS

The aim of this study was to investigate the impact of propeller emergence in severe waves, taking into account the coupling between the hull, propeller, and diesel engine dynamics. The main outcomes of the study for the selected ship are as follows:

- Propeller emergence has a significant influence on the fluctuation of all variables related to the hull, propeller, and engine.
- For a selected ship that was 182.880 m length with 9.782 m draught, and for a significant wave height of 3.260 m, the mean values of the three main variables of the system (i.e. ship speed, shaft angular velocity, and engine power) were 11.74 m/s, 9.711 rad/s, and 19,828 kW in calm water, which changed to 11.54 m/s, 9.705 rad/s, 19,473 kW in the propeller submerged condition, and to 10.34 m/s, 9.713 rad/s, and 13,287 kW in the propeller emerged condition. Hence, by including the propeller emergence, the variation in the ship speed and engine power was relatively high, while the change in the shaft angular velocity was negligible due to the use of a control strategy that maintained a constant shaft angular velocity via the governor.
- When Amp/Mean was used as a criterion, large fluctuations were observed for the propeller emergence conditions in waves. The values of Amp/Mean for the ship speed and engine power were 0.121 and 6.008 in submerged conditions, and these changed to 0.134 (+11%) and 7.912 (+32%) in the emerged condition. This confirms the high pulsatility of the engine power under both conditions.

- Based on the extent of variation, the system variables can be divided into three main groups showing low, moderate, and high fluctuations:
  – High fluctuation level: propeller torque, engine torque, delivered brake power, net thrust, and fuel rate;
  – Moderate fluctuation level: ship speed, advance number, and shaft angular velocity;
  – Low fluctuation level: flow and thermodynamic internal variables of the engine, such as the mass and temperature of the air accumulated in the inflow air manifold/receiver, the mass and temperature of the exhaust gases accumulated in the exhaust gas receiver, the mass flow rate of the exhaust gases after the cylinders and after the turbine of the turbocharger, the temperature of the combustion gases and the exhaust outflow gases from cylinders, etc.
- For a constant angular velocity of the engine shaft strategy, the fuel rate (and fuel index) under propeller ventilation conditions oscillates with a very high amplitude, from almost the minimum to the maximum permissible values, with almost the same frequency as the encounter frequency.

Declaration of competing interest

The authors declare that they have no known competing financial interests or personal relationships that could have appeared to influence the work reported in this paper.

REFERENCES

1. K. Rudzki, P. Gomulka, and A. T. Hoang, "Optimization model to manage ship fuel consumption and navigation time," *Polish Maritime Research*, 3 (115) vol. 29, pp. 141-153, 2022, doi: 10.2478/pomr-2022-0034.

2. T. T. Ngoc, D. D. Luu, T. H. H. Nguyen, and M. V. Nguyen, "Numerical prediction of propeller-hull interaction characteristics using RANS method," *Polish Maritime Research*, 2 (102) vol. 26, pp. 163-172, 2019, doi:10.2478/pomr-2019-0036.

3. M. B. Samsul, "Blade cup method for cavitation reduction in marine propellers," *Polish Maritime Research*, 2 (110) vol. 28, pp. 54-62, 2021, doi: 10.2478/pomr-2021-0021.

4. Y. Zhang, X. P. Wu, M. Y. Lai, G. P. Zhou, and J. Zhang, "Feasibility study of RANS in predicting propeller cavitation in behind-hull conditions," *Polish Maritime Research*, 4 (108) vol. 27, pp. 26-35, 2020, doi: 10.2478/pomr-2020-0063.

5. B. Lou and H. Cui, "Fluid–structure interaction vibration experiments and numerical verification of a real marine propeller," *Polish Maritime Research*, 3 (111) vol. 28, pp. 61-75, 2021, doi: 10.2478/pomr-2021-0034.

6. L. Guangnian, Q. Chen, and Y. Liu, "Experimental study on dynamic structure of propeller tip vortex," *Polish Maritime Research*, 2 (106) vol. 27, pp. 11-18, 2020, doi: 10.2478/pomr-2020-0022.

7. P. K. Quang, P. V. Hung, N. C. Cong, and T. X. Tung, "Effects of rudder and blade pitch on hydrodynamic performance of marine propeller using CFD," *Polish Maritime Research*, 2 (114) vol. 29, pp. 55-63, 2022, doi: 10.2478/pomr-2022-0017.

8. A. Nadery and H. Ghassemi, "Numerical investigation of the hydrodynamic performance of the propeller behind the ship with and without WED," *Polish Maritime Research*, (108) vol. 27, pp. 50-59, 2020, doi: 10.2478/pom r-2020 – 0065.

9. K. Koushan, "Dynamics of ventilated propeller blade loading on thrusters due to forced sinusoidal heave motion," in *Proceedings of the 26th Symposium on Naval Hydrodynamics*, Rome, Italy, 2006.

10. A. M. Kozlowska, S. Steen, and K. Koushan, "Classification of different type of propeller ventilation and ventilation inception mechanism," in *Proceedings of the First International Symposium on Marine Propulsors*, 2009.

11. K. Koushan, S. J. Spence, and T. Hamstad, "Experimental investigation of the effect of waves and ventilation on thruster loadings," in *Proceedings of the 1st International Symposium on Marine Propulsors (SMP'09)*, 2009.

12. A. Califano and S. Steen, "Analysis of different propeller ventilation mechanisms by means of RANS simulations," in *Proceedings of the First International Symposium on Marine Propulsors*, 2009.

13. M. Palm, D. Jürgens, and D. Bendl, "Numerical and experimental study on ventilation for azimuth thrusters and cycloidal propellers," in *Proc. 2nd Int. Symp. Marine Propulsors SMP*, 2011.

14. K. Koushan, S. Spence, and L. Savio, "Ventilated propeller blade loadings and spindle moment of a thruster in calm water and waves," in *Proceedings of the Second International Symposium on Marine Propulsors, SMP*, 2011.

15. A. M. Kozlowska, K. Wöckner, S. Steen, T. Rung, K. Koushan, and S. Spence, "Numerical and experimental study of propeller ventilation," in *Proceedings of the Second International Symposium on Marine Propulsors*, Hamburg, Germany, 2011.

16. K. J. Paik, "Numerical study on the performance of a partially submerged propeller in bollard condition," in *Proceedings of the Fifth International Symposium on Marine Propulsors (SMP'17)*, Session C, 2017.

17. C. Yvin, P. Muller, and K. Koushan, "Numerical study of propeller ventilation," in *Proceedings of the Fifth International Symposium on Marine Propulsors*, Espoo, Finland, 2017.

18. A. M. Kozłowska, "Hydrodynamic loads on marine propellers subject to ventilation and out of water condition," Norwegian University of Science and Technology (NTNU), 2019.

19. A. M. Kozlowska, Ø. Ø. Dalheim, L. Savio, and S. Steen, "Time domain modeling of propeller forces due to ventilation in static and dynamic conditions," *Journal of Marine Science and Engineering*, vol. 8, p. 31, 2020, doi: 10.3390/jmse8010031.

20. V. I. Lanchukovsky, "Safe operation of marine power plants," Institute of Marine Engineering, Science and Technology, 2009.

21. T. Szelangiewicz and K. Żelazny, "Prediction of the influence of propeller emergence on its thrust reduction during ship navigation on waves," 21 Scientific Journals of the Maritime University of Szczecin, pp. 83-87, 2010.

22. T. Szelangiewicz and K. Żelazny, "The influence of propeller emergence on the load of a marine engine of a ship sailing on irregular wave," Zeszyty Naukowe/Akademia Morska w Szczecinie, 2013.

23. G. Theotokatos and V. Tzelepis, "A computational study on the performance and emission parameters mapping of a ship propulsion system," in *Proceedings of the Institution of Mechanical Engineers, Part M: Journal of Engineering for the Maritime Environment*, vol. 229, pp. 58-76, 2015.

24. B. Taskar, "The effect of waves on marine propellers and propulsion," Norwegian University of Science and Technology (NTNU), 2017.

25. E. Tokgoz, P. C. Wu, S. Takasu, Y. Toda, "Computation and experiment of propeller thrust fluctuation in waves for propeller open water condition," Transactions of the Japan Society of Naval Architects and Ocean Engineers, vol. 25, pp. 55-62, 2017, doi: 10.2534/jjasnaoe.25.55.

26. Y. Kitagawa, O. Bondarenko, and Y. Tsukada, "An experimental method to identify a component of wave orbital motion in propeller effective inflow velocity and its effects on load fluctuations of a ship main engine in waves," *Applied Ocean Research*, vol. 92, p. 101922, 2019, doi: 10.1016/j.apor.2019.101922.

27. S. Naito, "Open water characteristics and load fluctuation of propeller at racing condition in waves," *J. Kansai Soc. Nav. Archit. Jpn.*, vol. 172, pp. 51-63, 1979.

28. K. Minsaas, O. Faltinsen, and B. Persson, "On the importance of added resistance, propeller immersion and propeller ventilation for large ships in a seaway," in *PRADS 83—2nd International Symposium on Practical Design in Shipbuilding,* Tokyo and Seoul, 17-22 Oct., 1983.

29. K. Minsaas K, H. Thon, and W. Kauczyński, "Influence of ocean environment on thruster performance," in *Proc. Int. Symp. Propeller and Cavitation*, 1986.

30. K. Koushan, "Environmental and interaction effects on propulsion systems used in dynamic positioning: An overview," in *Proceedings of the 9th International Symposium on Practical Design of Ships and other Floating Structures (PRADS)*, 2004.

31. Ø. N. Smogeli, "Control of marine propellers: From normal to extreme conditions," Norwegian University of Science and Technology (NTNU), 2006.

32. O. Bendarenko and K. Masashi, "Dynamic behaviour of ship propulsion plant in actual seas," *Marine Engineering*, vol. 45, pp. 1012-1016, 2010, doi.org/10.5988/jime.45.1012.

33. S. Saettone, "Ship propulsion hydrodynamics in wave," Danish Technical University (DTU), 2020.

34. H. Zeraatgar and M. H. Ghaemi, "The analysis of overall ship fuel consumption in acceleration manoeuvre using hull-propeller-engine interaction principles and governor features," *Polish Maritime Research*, vol. 26, pp. 162-173, 2019, doi: 10.2478/pomr-2019-0018.

35. M. H. Ghaemi and H. Zeraatgar, "Analysis of hull, propeller and engine interactions in regular waves by a combination of experiment and simulation," *Journal of Marine Science and Technology*, vol. 26, pp. 257-272, 2021, doi: 10.1007/s00773-020-00734-5.

36. E. M. Lewandowski, *The Dynamics of Marine Craft: Maneuvering and Seakeeping.* World Scientific, WSPC, 2004.

37. H. Zeraatgar, A. Moghaddas, and K. Sadati, "Analysis of surge added mass of planing hulls by model experiment," *Ships and Offshore Structures*, vol. 15, pp. 310-317, 2020, doi: 10.1080/17445302.2019.1615705.

38. B. Everitt, *The Cambridge Dictionary of Statistics*. Cambridge: Cambridge University Press, 1998.

39. M. H. Ghaemi, "Performance and emission modelling and simulation of marine diesel engines using publicly available engine data," *Polish Maritime Research*, 4 (112), Vol. 28, pp. 63-87, 2021, doi: 10.2478/pomr-2021-0050.

40. O. M. Faltinsen, "Prediction of resistance and propulsion of a ship in a seaway," in *Proceedings of the 13th Symposium on Naval Hydrodynamics,* Tokyo, 1980.

APPENDIX A

SURGE AND WAVE ORBITAL INFLOW VELOCITIES

The relationship between the advance speed and ship speed is defined by the mean wake fraction coefficient, $w(t)$, including the wave orbital inflow velocity, [26], as follows:

$$u_A(t) = [u(t) - \omega_e \bar{\eta}_1 \sin(\omega_e t - \varepsilon_1)](1 - w(t)) + \bar{u}_{PW} \cos(\omega_e t - kx_p \cos \mu) \tag{A.1}$$

where $\bar{\eta}_1$ and ε_1 are the amplitude and phase-lag of the surge motion, $\bar{u}_{PW}$ is the amplitude of the wave orbital inflow velocity, k is the wavenumber, x_P is the propeller x-coordinate and μ is the ship heading angle in respect to the wave direction. ω_e is the encounter frequency for sailing in deep waters, and is defined as follows:

$$\omega_e = \omega\left(1 - u\frac{\omega}{g}\cos\mu\right) \tag{A.2}$$

In [26], the authors have clearly shown that if λ/L (the wavelength divided by the ship's length) is less than one, then the surge speed effect is almost negligible. For the cases considered in this study, λ/L is less than one, and Eq. (A.1) can be represented as follows:

$$u_A(t) = u(t)(1 - w(t)) + \bar{u}_{PW} \cos(\omega_e t - kx_p \cos \mu) \tag{A.3}$$

MEAN-VALUE ZERO-DIMENSIONAL MATHEMATICAL MODEL OF THE DIESEL ENGINE

The details of the mean-value zero-dimensional mathematical model of the diesel engine are presented in [39], and a summary of the model is presented here. The model is divided into the following parts: turbine, compressor, turbocharger shaft, charge air cooler, intake air receiver, exhaust gas receiver and cylinders. The relevant equations are presented below, using the following nomenclature.

Letters:

A	area, equivalent area
c	specific heat coefficient
I	moment of inertia
k	coefficient
m	mass
M	torque (moment)
p	pressure
P	power
q	heat calorific value
R	gas constant
T	temperature
V	volume
Z	number of cylinders

Greek letters

η	efficiency
κ	adiabatic exponent
λ	coefficient
π	pressure ratio
ρ	density
ψ	flow function
ω	angular velocity

Lower indices

0	ambient condition
1	point before compressor
2	point after compressor
3	point after charge air cooler (before cylinders)
4	point after cylinders
5	point after turbine
am	air intake manifold (receiver)
at	atmosphere
b	burnt (fuel)
C	compressor
clr	charge air cooler
$comb$	combustion
$cr.$	critical
cyl	engine cylinders
E	engine
f	fuel
gr	exhaust gas receiver
$loss$	energy/power/torque losses
p	(at constant) pressure

T	turbine
TC	turbocharger
v	(at constant) volume
w	cooling water

Upper index

*	equivalent

Turbine:

$$\dot{m}_5 = A_T^* \cdot \psi_T \cdot \sqrt{P_{gr} \cdot \rho_{gr}} \tag{B.1}$$

where

$$\psi_T(\pi_T) = \begin{cases} \left[\dfrac{2\kappa_T}{\kappa_T - 1}\left(\pi_T^{\frac{2}{\kappa_T}} - \pi_T^{\frac{\kappa_T + 1}{\kappa_T}} \right) \right]^{\frac{1}{2}} & ;\ \pi_T \geq \pi_{T_{cr.}} \\[2em] \left[\kappa_T \cdot \left(\dfrac{2}{\kappa_T + 1} \right)^{\frac{\kappa_T + 1}{\kappa_T - 1}} \right]^{\frac{1}{2}} & ;\ \pi_T < \pi_{T_{cr.}} \end{cases} \tag{B.2}$$

and

$$\pi_{T_{cr.}} = \left(\frac{2}{\kappa_T + 1} \right)^{\frac{\kappa_T}{\kappa_T - 1}} \tag{B.3}$$

$$P_T = \dot{m}_5 \cdot \eta_T \cdot \frac{\kappa_T}{\kappa_T - 1} \cdot R_5 \cdot T_5 \cdot \left[1 - \pi_T^{\left(\frac{\kappa_T - 1}{\kappa_T} \right)} \right] \tag{B.4}$$

Compressor:

$$\dot{m}_1 = \dot{m}_1(\omega_{TC}, \pi_C, T_0) \quad \text{(compressor map)} \tag{B.5}$$

$$P_C = \frac{1}{\eta_C} \cdot \dot{m}_1 \cdot \frac{\kappa_C}{\kappa_C - 1} \cdot R_{at} \cdot T_{at} \cdot \left[1 - \pi_C^{\left(\frac{\kappa_C - 1}{\kappa_C} \right)} \right] \tag{B.6}$$

$$T_1 = \frac{1}{\eta_C} T_{at} \cdot \pi_C^{\frac{\kappa_T - 1}{\kappa_T}} \tag{B.7}$$

Turbocharger shaft:

$$J_{TC} \dot{\omega}_{tc} = M_T - M_C - M_{TC_{loss}} \tag{B.8}$$

Charge air cooler:

$$T_2 = T_1 - \eta_{clr} \cdot (T_1 - T_w) \tag{B.9}$$

Intake air receiver:

$$V_{am} \cdot \overset{\circ}{\rho}_{ia} = \dot{m}_1 - \dot{m}_3 \qquad \text{(B.10)}$$

$$\frac{dT_{am}}{dt} = \frac{1}{m_{am}}\left[\left(\frac{c_{p2}}{c_{vam}}\right) \cdot \dot{m}_2 \cdot T_2 - \left(\frac{c_{pam}}{c_{vam}}\right) \cdot \dot{m}_3 \cdot T_3 - T_{am} \cdot \dot{m}_{am}\right] \qquad \text{(B.11)}$$

Exhaust gas receiver:

$$V_{gr} \cdot \overset{\circ}{\rho}_{gr} = \dot{m}_4 - \dot{m}_5 \qquad \text{(B.12)}$$

$$\frac{dT_{gr}}{dt} = \frac{1}{m_{gr}}\left[\left(\frac{c_{p4}}{c_{vgr}}\right) \cdot \dot{m}_4 \cdot T_4 - \left(\frac{c_{pgr}}{c_{vgr}}\right) \cdot \dot{m}_5 \cdot T_5 - T_{gr} \cdot \dot{m}_{gr}\right] \qquad \text{(B.13)}$$

Engine cylinders and combustion process:

$$\dot{m}_3 = A^*_{cyl} \cdot \psi_{cyl}(\pi_{cyl}) \cdot \sqrt{p_3 \cdot \rho_3} \qquad \text{(B.14)}$$

$$\dot{m}_{combt} = \frac{\omega}{2\pi} \cdot V_{cyl} \cdot \rho_3 \cdot Z \qquad \text{(B.15)}$$

$$\eta_{fill} = 1 - exp(-k_b \cdot \lambda_b), \text{ where: } \lambda_b \approx \frac{\dot{m}_3}{\dot{m}_{combt}} \qquad \text{(B.16)}$$

$$\dot{m}_{comb} = \frac{\omega}{2\pi} \cdot Z \cdot V_{cyl} \cdot \frac{R_{am} T_{am}}{p_{am}} \cdot \left[1 - exp(-k_b \cdot \lambda_b)\right] \qquad \text{(B.17)}$$

where

$$\lambda_b = \frac{2\pi \cdot \dot{m}_3 \cdot R_{am} \cdot T_{am}}{\omega \cdot Z \cdot V_{cyl}} \qquad \text{(B.18)}$$

$$P_E = \eta_E \cdot \dot{m}_f \cdot q_f \qquad \text{(B.19)}$$

$$T_4 = T_{am} \cdot \frac{c_{p3}}{c_{p4}} \cdot \frac{\dot{m}_3 - \dot{m}_{comb}}{\dot{m}_4} + T_{comb} \cdot \frac{\dot{m}_{comb}}{\dot{m}_4} \cdot \frac{c_{pcomE}}{c_{p4}} \qquad \text{(B.20)}$$

where

$$T_{comb} = \frac{q_f \cdot \dot{m}_f \cdot (1 - k_{loss}) - P_E}{(\dot{m}_{comb} + \dot{m}_f) \cdot c_{p4}} + T_{am} \cdot \frac{\dot{m}_{comb}}{\dot{m}_{comb} + \dot{m}_f} \cdot \frac{c_{pam}}{c_{p4}} \qquad \text{(B.21)}$$

APPENDIX C

THREE MODELS OF THE THRUST DIMINUTION FACTOR, β

I. The first model was suggested in [28], and was based on the results presented in [40]:

$$\beta = \begin{cases} 0 & \varepsilon < -0.48 \\ 1 - 0.675(1 - 0.769\,\varepsilon)^{1.258} & ; \quad -0.48 \leq \varepsilon \leq 1.3 \\ 1 & \varepsilon > 1.3 \end{cases} \quad \textbf{(C.1)}$$

In this conservative relationship, thrust and torque reductions are expected to occur when the height of water above the propeller disc is less than 30% of the propeller radius.

II. The second model was put forward in [9]:

$$\beta \approx 0.5 + 0.5(min(max(\varepsilon, -1), 1)) \quad \textbf{(C.2)}$$

This equation is a linear approximation of Eq. (C.1), and can be applied to simplify the calculations in the steady-state condition.

III. In [32], β is defined as follows:

$$\beta = \begin{cases} a(\varepsilon + b) & ; \varepsilon \leq A \\ 1 & ; \varepsilon > 1 \end{cases} \quad \textbf{(C.3)}$$

where

$$A = 1.8 - 0.95\,J \quad \textbf{(C.4)}$$

$$b = \frac{1 - a\,A}{a} \quad \textbf{(C.5)}$$

and a is obtained in a loop based on the propeller disc area ratio. To apply this relationship initially, it is necessary to calculate a using Eq. (14):

$$a = \frac{\beta - 1}{\varepsilon - A} \quad \textbf{(C.6)}$$

then b from Eq. (C.5), and finally calculate β according to Eq. (C.3). Although this method includes the advance number, the results for typical values of the advance number are the same as those obtained from Eq. (14).
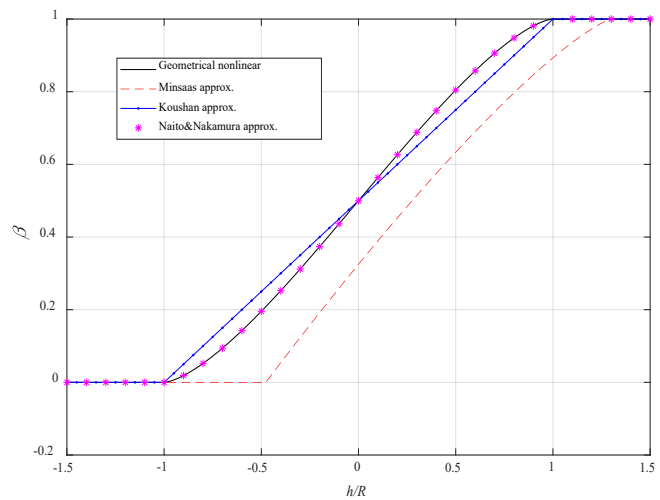
The methods reviewed above are compared in Fig. C.1.

Fig. C.1. Comparison of thrust diminution factor, β, calculated using three different methods

In [18], the problem of propeller ventilation was investigated in detail, and an advanced analytical and numerical model for calculating β was proposed. Review of this study is recommended whenever hydrodynamic aspects of propeller ventilation are concerned, and particularly when the loads, moments, and thrust and torque coefficients should be included in the analysis.

CONTACT WITH THE AUTHORS

Mohammad Hossein Ghaemi
e-mail: ghaemi@pg.edu.pl

Gdańsk University of Technology
Faculty of Mechanical Engineering and Ship Technology
Gdańsk
Poland

Hamid Zeraatgar

Amirkabir University of Technology
Faculty of Maritime Technology
Iran